THE EFFECT OF SURFACE ACTIVE SUBSTANCE CONCENTRATION ON THE PROPERTIES OF FOAMED AND NON-FOAMED GYPSUM

ZORA BAZELOVÁ[#], LADISLAV PACH, JÁN LOKAJ

Department of Ceramics, Glass and Cement, Faculty of Chemical and Food Technology,
Slovak Technical University, Radlinského 9, Bratislava, Slovakia

[#]Corresponding author, e-mail: zora.bazelova@stuba.sk

Foamed gypsum was prepared by the direct foaming method. Properties of foamed and non-foamed gypsum were investigated using plaster suspension containing surface active substance (SAS). Since SAS has amphiphilic properties its solutions are prone to foaming. The combination of foaming and the hydration of calcium sulphate hemihydrate ($CaSO_4.1/2H_2O$) led to fast solidification, resulting in strong, porous bodies. Bulk density, compressive strength and the pore size varied markedly depending on both the quantity of SAS and water/plaster weight ratio. Bulk density of the foamed gypsum ranged from 0.20 to 0.58 g/cm^3 and the pore size reached 50 μm to 1.3 mm depending on the concentration of the surfactant. The compressive strength of the foamed gypsum and the non-foamed one increased with increasing bulk density. The dried non-foamed gypsum showed high compressive strengths up to 12 MPa.

INTRODUCTION

Foamed gypsum belongs to ceramic foams. Ceramic foams can be applied in many different fields of technological processes. These include filters, membranes, lightweight building materials, thermal and acoustic insulation, catalysis, etc. In these applications ceramic foams can be used because of their properties such as high porosity, high surface area, low density, low thermal conductivity, high permeability, high temperature stability, chemical inertness, etc. [1-4].

The processing method has a decisive influence on both the microstructure and properties of the material [5]. The most conventional process for producing ceramic foams is the replica technique which consist in impregnation of a polymeric sponge with a ceramic slurry, pyrolysis of the polymeric substrate, and finally sintering for solidification of the foam. This technique allows to prepare ceramic foams with pore sizes ranging from 200 μm to 3 mm at the porosity levels between 40 % and 95 % [2]. An alternative method for obtaining the ceramic foam is the direct foaming method. The direct foaming method offers an easy, cheap and fast way to prepare porous ceramics with open or closed porosities varying from 40 % to 97 % and pore sizes varying from 30 μm to 1.2 mm [2]. In this method ceramic foams are produced by incorporating a gaseous phase into a ceramic suspension or liquid media. The incorporation of the gaseous phase is carried out either by mechanical frothing, injection of a gas stream, gas-releasing chemical reactions or solvent evaporation [6].

Wet foams are thermodynamically unstable systems due to their high gas-liquid interfacial area. In wet foams several physical processes take place which decrease the overall system free energy leading to foam destabilization. The main destabilization mechanisms are drainage, coalescence and disproportionation [7]. In wet foam the presence of a surface active agent or surfactant is necessary to stabilize the foam. Surfactants are chemical compounds typically long-chain molecules that are amphiphilic [5]. The most favourable orientation of these molecules is on surfaces or interfaces so that each part of the molecule can reside in the fluid for which they have greater afinity. Surfactants contain a polar (hydrophilic) head group and a non-polar (hydrophobic) chain tail which therefore accumulate on the surface of the liquid, thus reducing the surface tension. Ceramic foams stabilized by surfactants are reported to have pore sizes ranging from 35 μm up to the mm scale [2].

The aim of this work was to investigate the possibility of using the surface active substance as a foaming agent to prepare the foamed gypsum. Wet foams stabilized with surfactants collapse after foaming within a several minutes. Plaster is the one of the main minerals – based hydraulic binders. It helps to maintain a stable foam that spontaneously hardens and thus prevents

the foam from collapsing. Setting and hardening of plaster ($CaSO_4 \cdot 1/2H_2O \rightarrow CaSO_4 \cdot 2H_2O$) takes place in continous elementary steps: a.hemihydrate dissolution, b.dihydrate crystals nucleation and c.growth of dihydrate crystals [8]. The dihydrate forms a saturated solution in the aqueous suspension. Simultaneously, the germs of the former are being produced in the form of the needle-like shape crystals.

EXPERIMENTAL

Aqueous suspensions containing plaster powder ($CaSO_4 \cdot 1/2H_2O$, BPB Formula GmbH Walkenried, Germany), deionized water and the surface active substance (SAS, Procter & Gamble, Rakovnik, Czech Republic) as a foaming agent containing 5-15% anionic surfactants and <5% nonionic surfactants were prepared. SAS is a comercial product the base of which is sodium lauryl sulphate. Plaster powder was added to water containing SAS. The samples of plaster were prepared using a consistency (water/plaster weight ratio) of 0.60, 0.66, 0.72 and 0.78. Typical water/dry materials weight ratio in building applications is 0.68 [9]. The SAS quantity was less than 2.2% of the overall substance mass (Table 1).

Table 1. Composition of the gypsum samples prepared: water/plaster weight ratio (constant plaster weight = 166.7 g), quantity of SAS (4, 5, 6 g) and the content of SAS in suspensions, *1-16* - number of samples.

water/plaster weight ratio	quantity of SAS (g)			
	0	4	5	6
	SAS (wt.%)			
0.60	*1* 0.00	*2* 1.48	*3* 1.84	*4* 2.20
0.66	*5* 0.00	*6* 1.42	*7* 1.77	*8* 2.12
0.72	*9* 0.00	*10* 1.38	*11* 1.71	*12* 2.05
0.78	*13* 0.00	*14* 1.33	*15* 1.66	*16* 1.98

Aqueous suspensions were prepared

1. mixed in a laboratory mixer at a mixing velocity of cca. 800 rpm for 1.5 min (foamed samples).
2. hand-mixed for cca. 1.5 min (non-foamed samples).

Initial samples were mixed for 1 to 2 minutes to determine the optimum mixing time. Hardening of the plaster is determined by the mixing time. The mixing must be completed before the hardening starts. The material microstructure is breaking during the longer mixing time. Non-homogenous porosity of samples is caused by the short mixing time due to low foaming (high bulk density). As a result, the optimal mixing time was determinated being up to 90 ± 10 sec. This mixing time was thus used to prepare all samples.

Hardening of the plaster was monitored by measuring the temperature of the samples during 40 minutes.

For this purpose, 500 ml of wet foam was poured out into a plastic container into which a digital thermometer sensor was inserted.

All experiments were performed at the laboratory temperature of 295±1 K. The resulting wet foams were put into cylindrical forms with diameters of 130 mm and lengths of 30 mm. All foams were initially dried at laboratory temperature for approximately 5 days. After the consolidation, the samples were dried at 323 K to constant weight. The bulk density of the foams was calculated from the weight-to-volume ratio. Compressive strength measurements were performed on the universal testing machine (Hegewald & Peschke, Nossen, Germany). Cylindrical samples with diameters of 17 mm and lengths of 30 mm were drilled out of the piece of the foam with a core drill. Samples were crushed under a compression of 5 mm/min. Microstructure was observed by scanning electron microscopy (SEM, TESLA BS 300). Afterwards, foamed gypsums were cut and pore size distribution were directly obtained from planar section.

RESULTS AND DISCUSSION

Temperature profile of plaster hardening

When plaster is mixed with water, the ensuing hydration reaction is highly exothermic [10]. Under given conditions the kinetics of the plaster hardening depends on both temperature and its composition, and also on the way experiment was carried out (the way of mixing). As can be seen from Figure 1, all courses are similar. Temperature risis to the maximum and then it decreases steadily [10]. The processes are faster in the foamed samples than that in the non-foamed ones. Temperature courses of the foamed samples are practically identical for all three SAS quantities. This may be explained by
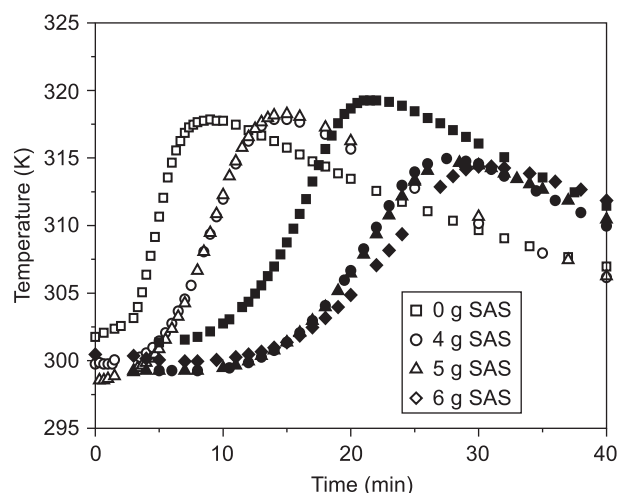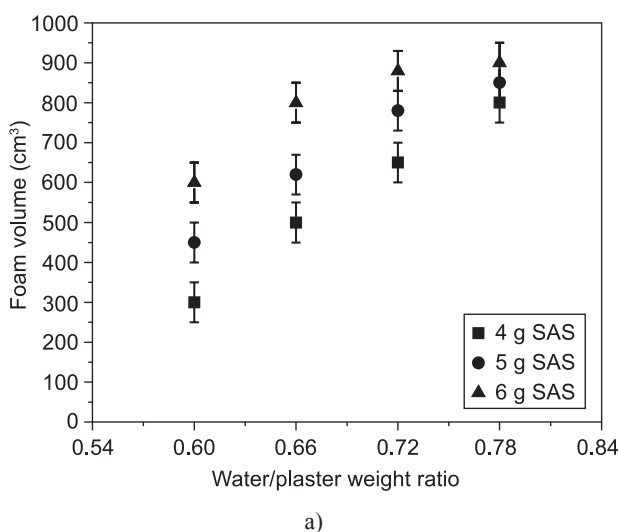
Figure 1. Dependence of the temperature (foamed ◊ □ ○ Δ, non-foamed samples ♦ ■ ● ▲) on the time of hardening, on the way of mixing and on the SAS quantity.

small differences in weight fraction of the foaming agent in the system. Nevertheless, it can be seen that with increasing quantity of SAS the rate of plaster hardening slows down [11]. This trend also applies to non-foamed samples (Figure 1).

The observed result can be explained by: 1.the SAS quantity causes slowing down the crystal growth of $CaSO_4 \cdot 1/2H_2O$ 2. the SAS quantity slows down the dissolution of $CaSO_4 \cdot 2H_2O$. Both phenomena can be explained in terms of SAS being absorbed onto the surfaces of both hydrates. The mixing speed in both cases (foamed and non-foamed gypsum), however, affects the process of plaster hardening. The faster mixing speeds up dissolving of $CaSO_4 \cdot 1/2H_2O$ and the crystal growth of $CaSO_4 \cdot 2H_2O$ as well. The outcome of this study suggests that both the SAS quantity and the mixing speed decrease the rate of hydration [11].

Bulk density of hand-mixed samples (non-foamed) shows the same trend as that of the foamed one.The measured bulk densities of the non-foamed gypsum are given in Table 2. On increasing both the water/plaster weight ratio and the quantity of SAS, the bulk density of non-foamed gypsum decreases.

Table 2. Non-foamed gypsum bulk density dependency on the suspension composition, *1-16* - number of samples.

water/plaster weight ratio	quantity of SAS (g)			
	0	4	5	6
	bulk density (g/cm^3)			
0.60	*1* 1.128	*2* 1.080	*3* 1.067	*4* 1.054
0.72	*9* 1.004	*10* 0.982	*11* 0.976	*12* 0.973
0.78	*13* 0.973	*14* 0.929	*15* 0.928	*16* 0.903

Bulk density of foamed gypsum

The quantity of foaming agent and the water/plaster weight ratio affected the foam volume, the results of which is the sample final bulk density [12] as shown in Figure 2. On increasing the quantity of foaming agent the wet foam volume increases with constant mixing time. On increasing the water/plaster weight ratio the difference among the foam volumes decreases as a consenquence of greater dilution and thus due to the smaller weight fraction of the foaming agent (Figure 2a). On increasing the wet foam volume bulk density decreases due to the larger volume of gaseous phase in the system. The bulk densities of the foamed gypsum ranged from 0.21±0.01 g/cm^3 to 0.56±0.02 g/cm^3, depending on the water/plaster weight ratio and on the quantity of SAS (Figure 2b). The results obtained fit well with those given in [12, 13].

Compressive strength of foamed
and non-foamed gypsum

Figure 3 shows a typical stress-strain curve for the set plaster [9] and ceramic foams [14] under compression testing. After the contact cross-head had contacted the sample the load increased. When the applied load exceeded the maximum value the sample started crushing. In the non-foamed gypsum a much higher maximum stress value was reached than that in the foamed one (Figure 3). After this point, the compressive strength decreases sharply in the non-foamed gypsum due to the rupture of the sample along its entire height (Figure 3a) but the compressive strength remains constant or decreases slightly in the foamed one due to its porosity (Figure 3b).
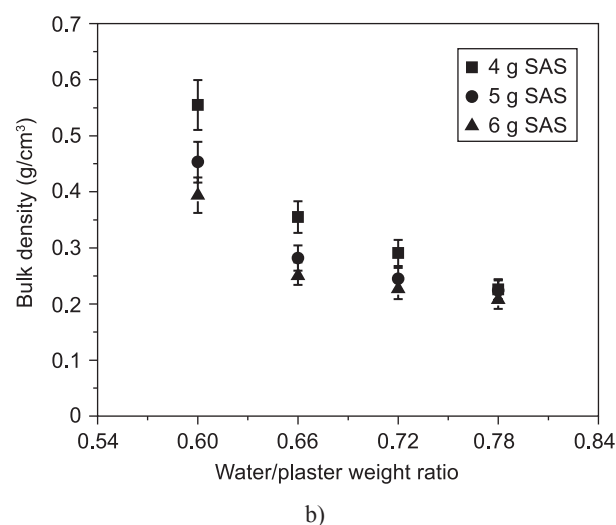

a)

b)

Figure 2. Effect of surfactant quantity and water/plaster weight ratio on the foam volume (a), and on the bulk density of foamed gypsum (b).
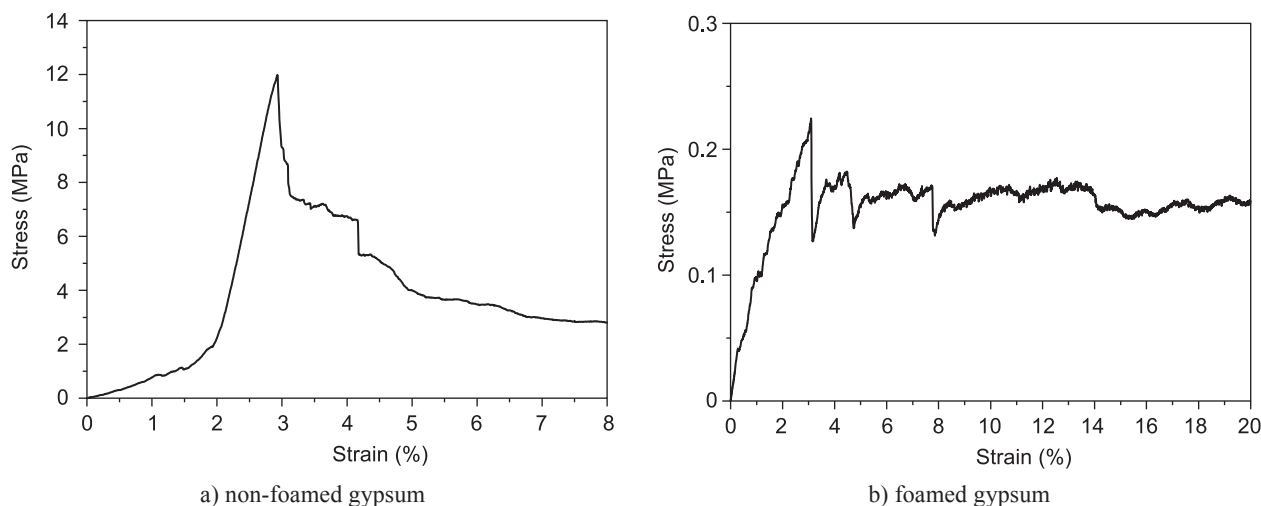
Figure 3. Typical stress-strain curves for non-foamed gypsum (sample No.9) (a), and for foamed one (sample No. 10) (b).

Three measurements of the compressive strength for each sample (Figure 4, sample No. 6) were carried out. For the approximate expression, the stress-strain curves were calculated by use of polynomial regression (Figure 4). The aim of the regression was to find a function which would fit best to describe the curves (6th degree polynomial). For each regression the coefficient of determination (R^2) was calculated. Coefficient of determination (R^2) is a statistical measure of how well the regression line matches the real data points. It can be interpreted as the percentage of the variance shared by the sets of numbers. The coefficient of determination was 72-98%. The high values of the determination coefficient indicate that the stress-strain curves of the foamed gypsum can be described by the polynomial function.

Figure 5 shows the compressive strength of the foamed gypsum with different water/plaster weight ratio and with different quantity of the surfactant. The increase of the SAS quantity and simultaneously at the same water/plaster ratio causes the decrease of the hardened gypsum strength [15]. In the foam the SAS acts as a lubricant which allows the mutual displacement of $CaSO_4 \cdot 2H_2O$ crystals and the compression of the sample without crash.

The density plays an important role in determining the mechanical properties of foams [16, 17]. The compressive strength of the foams increased with the increasing bulk density. The increases of the SAS quantity and the water/plaster weight ratio causes the decrease of the hardened foamed gypsum strength (Figure 5). The results obtained fit well with that given in [12]. Small differences can be ascribed to different ways to the foam preparation. Non-foamed gypsum shows the same trend (Table 3). Compressive strength exceeds its maximum without surfactant.
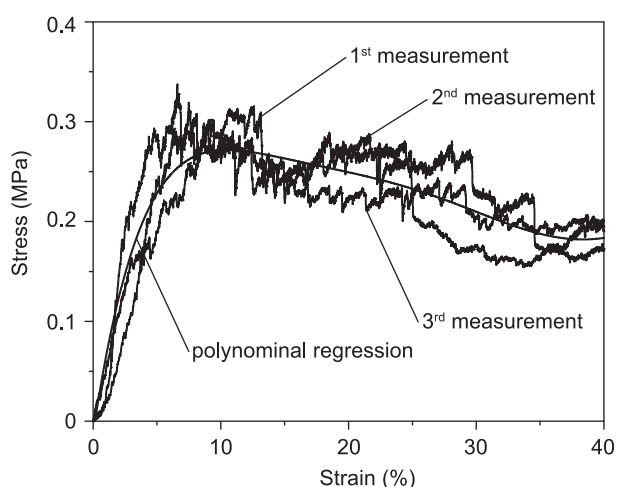

Figure 4. Polynomial – regression fit for the compressive stregth of three stress-strain curves (3 parallel measurements) for the foamed gypsum (sample No. 6), R^2 = 93.27 %.
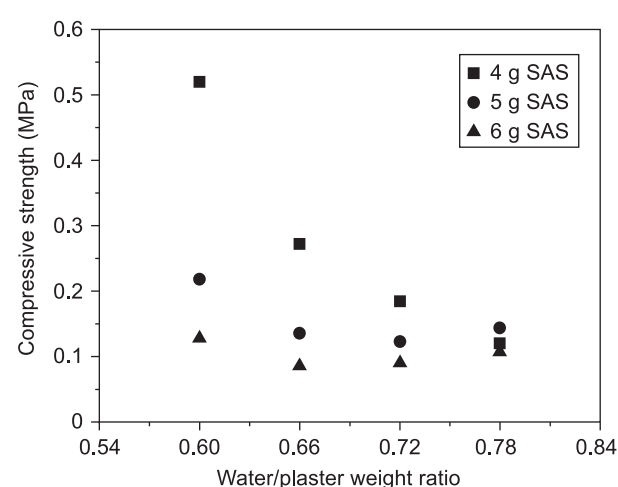

Figure 5. Compressive strength of foamed gypsums containing different amount of SAS as a function of water/plaster weight ratio.

Table 3. The maximum compressive strenght of the hand-mixed gypsum (non-foamed sample), *1-16* - number of samples.

water/plaster weight ratio	quantity of SAS (g)			
	0	4	5	6
	compressive strenght (MPa)			
0.60	*1* 8.809	*2* 8.256	*3* 7.442	*4* 5.417
0.72	*9* 6.853	*10* 5.297	*11* 4.545	*12* 3.699

Microstructure of foamed gypsum

Figure 6 shows the microstructure of the foamed gypsum obtained after drying. Diameters of approx. 100 pores were measuered using SEM. The average pore diameter was calculated by dividing the visible average pore diameter on the 2D cross section by 0.79 [18].

As can be seen in Figure 6 the pore size decreases with increasing concentration of the surfactant. This is also quantitatively described in Figure 7 where pore sizes ranging from 0.05 to 0.35 mm with their distribution for the systems investigated are shown.

Thick needle-like shape crystals and larger particles are formed during plaster hydration (Figure 8). The orientation of crystals in non-foamed gypsum is randomly (Figure 8a, b). The size and formation of crystals of $CaSO_4.2H_2O$ decreases with increasing SAS concentration. Consequently, the nucleation of $CaSO_4.2H_2O$ in the system increases. It appears that the SAS modify the process of nucleation by changing the solution saturation/supersaturation [10].The orientation of the crystals in the foamed gypsum is randomly just in the Plateau border (Figure 8c). On the origin interface

liquid - gas there is ordering of crystals onto the surface planar section (Figure 8d). The mixing speed affects the size of the crystals. The crystals are longer at hight speed mixing than that produced by the hand-mixing (Figure 8b, d).

CONCLUSION

The aim of this work was to investigate the influence of surfactant quantity and water/plaster weight ratio on the properties of foamed and non-foamed gypsum.
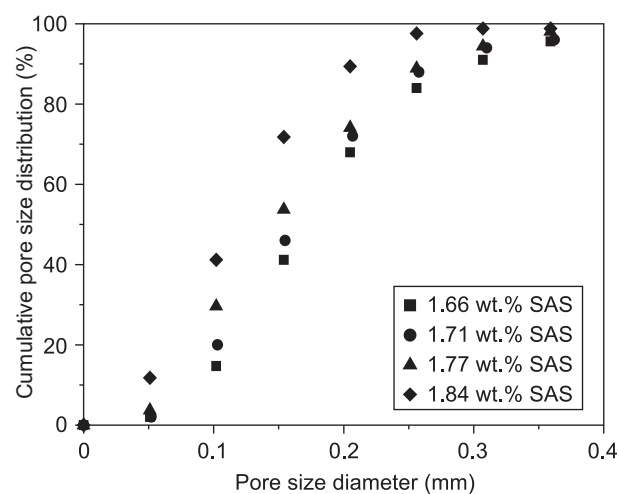

Figure 7. Cumulative pore size distribution of foamed gypsum prepared from suspensions containing different concentrations of SAS.
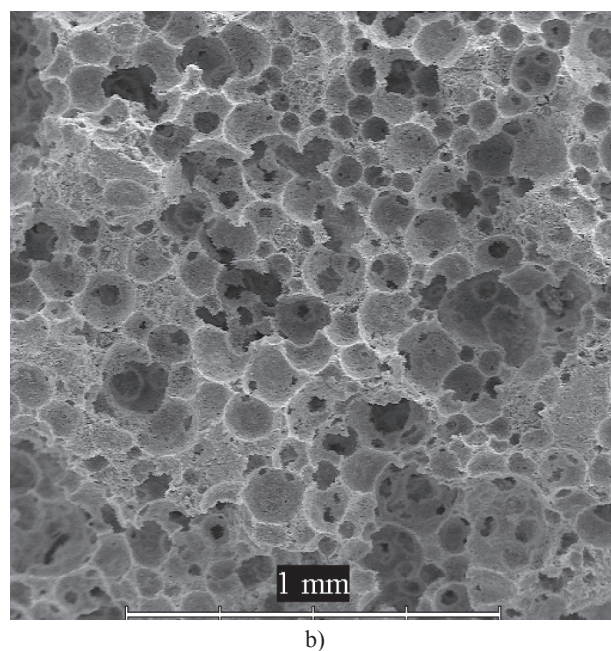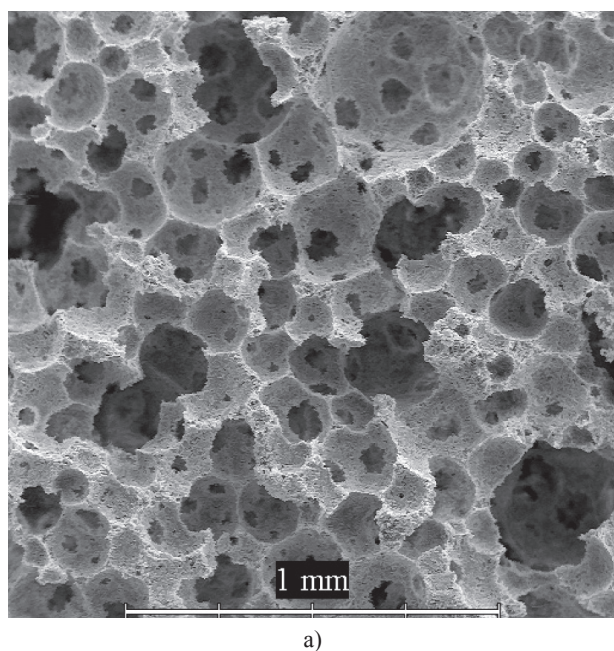

a)

b)

Figure 6. SEM images of pores containg different concentration of the surfactant (a) 1.98 wt.% - sample No. 16 (b) 2.12 wt.% - sample No. 8.

Foamed gypsum was prepared by the direct foaming method. A small change in SAS concentration proved a major influence on the bulk density of the samples. On increasing the SAS quantity the bulk density decreases, samples being more fragile and thus they have lower compressive strength. The bulk density of the foamed gypsum can be varied by altering the foam volume. Incorporation of air into the system influenced all measured parameters. Foamed gypsum shows a lower bulk density and lower compressive strength than the non-foam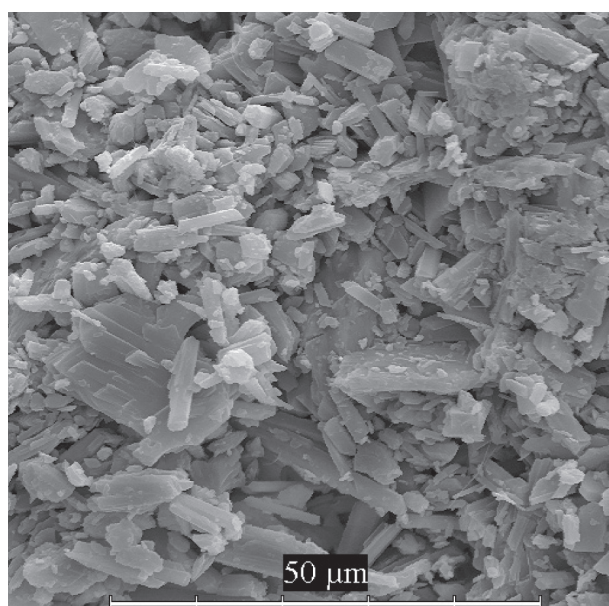ed one. Orientation of the crystals in the foamed gypsum is randomly just in the Plateau border. On the origin liquid - gas interface there is an ordering of crystals onto the surface planar section.
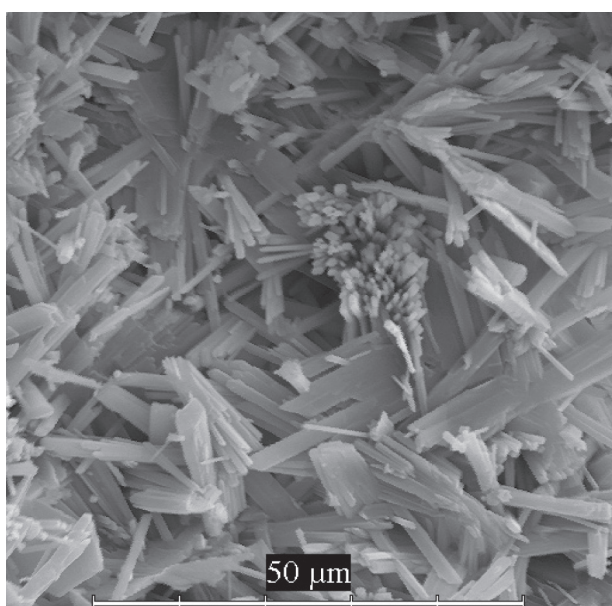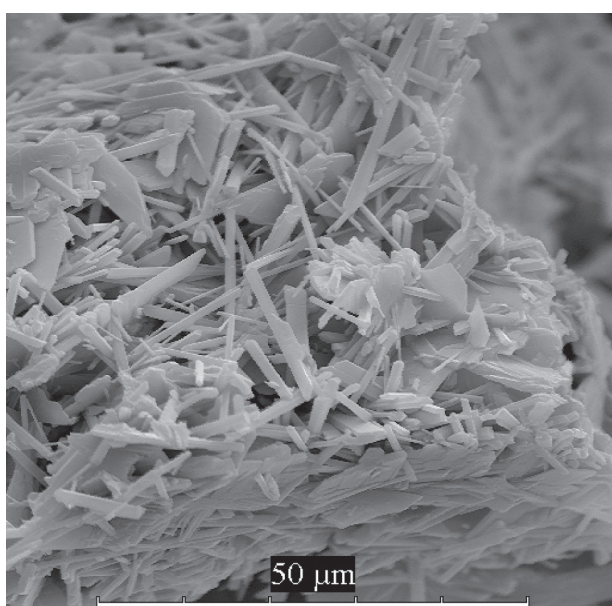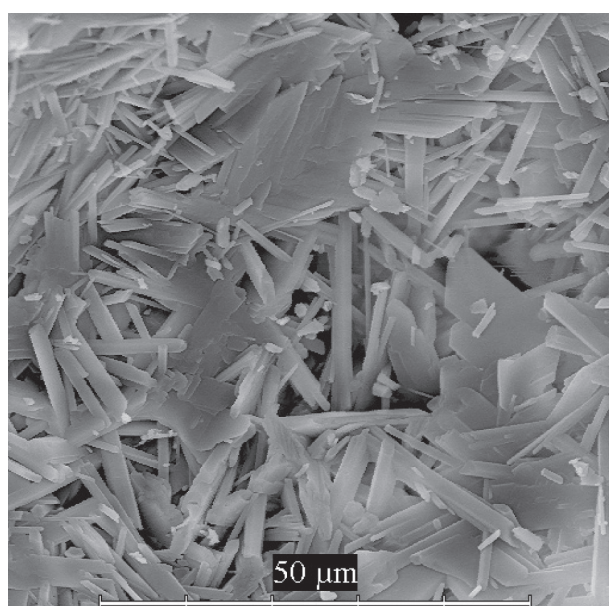
Figure 8. SEM microstructure of gypsum crystals, non-foamed gypsum - 0 wt.% SAS – sample No. 13 (a) non-foamed gypsum - 1.98 wt.% SAS – sample No. 16 (b) foamed gypsum – Conflict point of pores- plateau border (c), foamed gypsum - the area's origin interface liquid-gas- 1.98 wt.% SAS – sample No. 16 (d).

References

1. Sepulveda P., Binner J.G.P.: Journal of the European Ceramic Society *19*, 2059 (1999).
2. Studart A.R., Gonzenbach U.T., Tervoort E., Gauckler L.J.: Journal of the American Ceramic Society *89*, 1771 (2006).
3. Montanaro L., Jorand Y., Fantozzi G., Negro A.: Journal of the European Ceramic Society 18, 1339 (1998).
4. Colombo P., Bernardo E.: Composites Science and Technology *63*, 2353 (2003).
5. Barg S., Soltmann CH., Andrade M., Koch D. et al.: Journal of the American Ceramic Society *91*, 2823 (2008).
6. Gonzenbach U.T., Studart A.R., Tervoort E., Gauckler L.J.: Journal of the American Ceramic Society *90*, 16 (2007).
7. Brent S.M., Rammile E.: Current Opinion in Colloid & Interface Science *9*, 314 (2004).
8. Hlaváč J.: *Základy technologie silikátů*, 2nd ed., p.439-441, SNTL, Prague 1981 (in Czech).
9. Eve S., Gomina M., Gmouh A., Samdi A. et al.: Journal of the European Ceramic Society 22, 2269 (2002).
10. Singh N.B., Middendorf B.: Progress in Crystal Growth and Characterization of Materials *53*, 57 (2007).
11. Rajabipour F., Sant G., Weiss J.: Cement and Concrete Research *38*, 606 (2008).
12. Çolak A.: Cement and Concrete Composites *22*, 193 (2000).
13. Akthar F.K., Evans J.R.G.: Cement and Concrete Research *40*, 352 (2010).
14. Peng H.X., Fan Z., Evans J.R.G.: Ceramics International 26, 887 (2000).
15. Skujans J., Vulans A., Iljins U., Aboltins A.: Applied Thermal Engineering *27*, 1219 (2007).
16. Gibson L. J.: Journal of Biomechanics *38*, 377 (2005).
17. Brothers A, H., Dunand D. C.: Materials Science and Engineering A *489*, 439 (2008).
18. Williams A. M., Garner C. P.: Journal of the American Ceramic Society *91*, 3113 (2008).